ChemPubSoc Europe

DOI: 10.1002/celc.201700464

CHEMELECTROCHEM Articles

Special Issue

Ionic Transport in Microhole Fluidic Diodes Based on Asymmetric Ionomer Film Deposits

Klaus Mathwig,*[a] Barak D. B. Aaronson,[b] and Frank Marken*[b]

Microhole fluidic ionic diodes based on asymmetric deposits of charged ionomer membranes (e.g. Nafion or polymers of intrinsic microporosity) on microhole supports yield high rectification ratios for ionic transport. They are fabricated without the need for complex micro- or nanostructuring, and show potential for future applications in desalination and biosensing. Here, we propose an explanation for the functional principle for this type of materials-based ionic diode. A predictive computational model for ionic diode switching is based on finite element analysis. It is employed to determine the influence of diode geometry as well as type and concentration of aqueous electrolyte on the rectification behavior.

1. Introduction

Nanofluidic devices[1] are important in sensing,[2] in energy conversion,[3] and in scanning electrochemical microscopies (SECMs).[4] With an applied potential across the nanofluidic device, ionic rectifier or "ionic diode" effects[5] are observed when charge transport occurs asymmetrically, i.e., when a component of the nanofluidic device introduces asymmetry.[6] Although mechanistic details for rectification are subtle, asymmetry has been introduced in various ways including nano-cone devices,[7,8,9] varying channel surface charges,[10,11] in gel-gel junctions,[12] by operating devices in contact with two different electrolyte media,[13] or by a precipitation reaction.[14] Recently, it has been shown that polymers of intrinsic microporosity (PIMs) deposited asymmetrically onto a microhole in poly-ethylene-terephthalate (PET) also show ionic diode characteristics.[15,16]

Potential areas for applications of ionic diodes are in biosensing,[17] "iontronics",[18] in energy harvesting,[19,20] and in desalination.[21] However, ionic diode devices often require extensive microfabrication which limits practicality and scale up. Recently, it was shown that also porous materials in bulk as a highly charged ionomer film membranes show good rectification behavior when placed asymmetrically on a micrometer sized hole.[22] This approach largely eliminates the necessity for complicated micro- or nanofabrication. Rectification of ionic transport in similar devices has now been shown for a variety of porous charged films materials including Nafion[23] and reconstituted cellulose.[24] The rectification effect was generally attributed to electrokinetic effects, related to those which have previously been observed in nanochannel diodes,[25] in nanopipettes/nanocones,[8] and in microfluidic channel devices.[26,27] For these configurations, ionic rectification could usually be well-modelled and predicted using a Poisson-Nernst-Planck (PNP) formalism, which is employed here also for the microhole-ionomer diode. Work by Yossifon and coworkers has been reported on electrolyte/ionomer-filled micro-channels.[28,29]

Figure 1 shows a typical experimental configuration with the highly charged ionomer (here Nafion[24]) coating on a microhole facing the working electrode. When current-voltage curves are recorded, cations and anions are driven from the bulk reservoirs through the ionomer film and micro-orifice. A clear switch from a closed state (negative) to an open state (positive, see Figure 1B) is observed with high current rectification factor of up ~30 (depending on the geometry of the deposit).

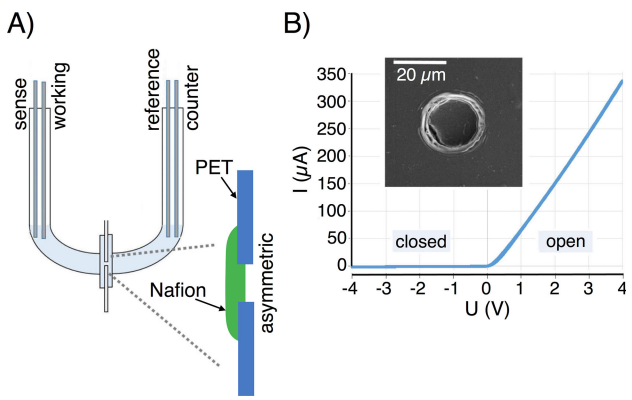

Figure 1. A) Schematic drawing of the four-electrode experimental configuration with an ionomer membrane asymmetrically deposited onto a microhole in PET facing the working electrode. B) Typical *I–V* curve (scan rate 10 mV s^{-1}; aqueous 10 mM HCl on both sides), showing a closed and open diode. The inset shows and electron micrograph of the 20 μm diameter microhole filled with Nafion (imaged from the PET side).

[a] *Dr. K. Mathwig*
University of Groningen
Groningen Institute of Pharmacy
Pharmaceutical Analysis
P.O. Box 196, 9700 AD Groningen, The Netherlands
E-mail: k.h.mathwig@rug.nl
[b] *Dr. B. D. B. Aaronson, Prof.Dr. F. Marken*
Department of Chemistry
University of Bath
Claverton Down, Bath BA2 7AY, UK
E-mail: f.marken@bath.ac.uk

Supporting information for this article is available on the WWW under https://doi.org/10.1002/celc.201700464

Special Issue *An invited contribution to the Alan Bond Festschrift*

Here, a *functional explanation* is developed for the rectification effect observed for asymmetric ionomer film deposits on a microhole. It is based on a change of conductivity of the diode due to accumulation or depletion of charge carriers in the microhole.

2. Results and Discussion

2.1. Diode Working Principle

Figure 2A shows a proposed model for current rectification. A non-conductive membrane (dark blue) with a single micron-sized orifice separates two reservoirs with equal concentrations of electrolyte ions (such as H^+, Cl^- or Na^+, OH^-). On the left side of this microhole an ionomer with nanoscale-porosity is deposited, it partially extends into the microhole. The nanopores exhibit a high surface charge exceeding the charge density in the bulk electrolyte (e.g., a $-150\ kC\,dm^{-3}$ for Nafion corresponding to an 'excess charge carrier concentration' of

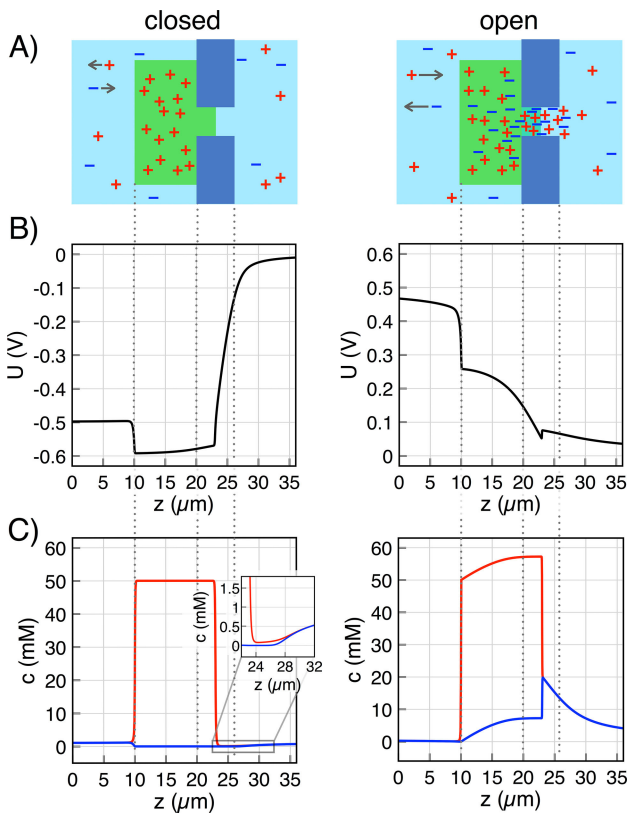

Figure 2. Diode behavior for an asymmetric film deposit with a negative net charge (green area) for forward bias (left) and reverse bias (right) for a 1 mM electrolyte concentration, 50 mM fixed $-e^-$ in the ionomer, a cylindrical micropore with 10 μm diameter and bias of +/−0.5 V at the left reservoir. A) Schematic representation of ion distribution of mobile ions. B) Potential distribution. C) Cation and anion distribution. The fixed negative charge concentration of 50 mM in the range of 10 to 26 μm are not shown. The inset in (C) is a magnification of the microhole area. In forward bias, ions accumulate in the electrolyte-containing part of the microhole ($z = 23..26$ μm), whereas in reverse bias the electric potential drops mainly in this segment, leading to current blockage by depletion of cations and anions.

1.5 $mol\,dm^{-3}$ [23,30]) and a lower mobility of charge carriers. Electrolyte ions are transported by diffusion as well as by migration in an electric field determined by the potential of electrodes positioned in both reservoirs.

Ion rectification is determined and dominated by the conductivity within the electrolyte-containing segment of the microhole. The bulk reservoirs *cannot* limit the current due to their large volume and high number of charge carriers. Within the porous ionomer membrane, conductivity is also high: While mobility of ions is reduced as compared to the bulk, the density of fixed surface charges is orders of magnitude higher than in the bulk, reducing also the electric potential in the ionomer. These fixed charges are counterbalanced by the same high amount of mobile counter ions drawn into the membrane, and, thus, its overall conductivity is high. Experimentally, this membrane conductivity is demonstrated by the comparatively high electrical resistance of a completely open micropore without any film deposit.[23]

Rectification is caused by the following effect (for the example of a negatively charged membrane as shown in Figure 1): In reverse bias, ions are electrophoretically driven out of the micropore, i.e., anions towards the anode counter electrode on the right, and cations through the ionomer membrane towards the cathode working electrode in the left reservoir. Removed anions cannot be readily be replenished from the ionomer film because almost exclusively fixed negative charges and an equal amount of positive mobile charge carriers are present there. This leads to two effects: The applied electric field drops predominantly in the solution-filled part of the micropore (see $z = 23..26$ μm in Figure 1B, Left side), and this segment is depleted of ions (see Figure 1C, Left side and Inset). Consequently, the current is blocked. In forward bias, on the other hand, anions are driven into the micropore from the right side, and cations from the ionomer on the left. Now, a high concentration of mobile cations is available in the ionomer membrane, and anions are hindered from leaving the microhole towards the anode on the left by the highly negatively charged membrane. Hence, the potential gradient in the micropore is small, ions accumulate (see Figure 1B, C, Right side), and the current is high.

2.2. Transport Model

To numerically model potential and concentration gradients in the microfluidic diodes we use the same PNP formalism used for nanofluidic diodes.[31,32] The electric potential is the described by the Poisson equation [Eq. (1)]:

$$\varepsilon_r\varepsilon_0\Delta\varphi = -\frac{\rho}{\varepsilon_r\varepsilon_0} \quad (1)$$

Here, φ is the electric potential, ρ the space charge density and $\varepsilon_r\varepsilon_0$ the electric permittivity ($\varepsilon_r = 80$ everywhere). A potential of $\varphi = -0.5\ldots0.5$ V is applied at the outer boundary of one reservoir (left side in Figure 1A), while the a reservoir boundary on the right side is kept constant at $\varphi = 0$ V. Ion flux

densities N are calculated by the simplified Nernst-Planck equations (in absence of drift and a magnetic vector potential) for cations and anions with the concentrations c_{cat} and c_{an} [Eq. (2)]

$$N_{cat} = -D_{cat}\nabla c_{cat} - u_{cat}z_{cat}Fc_{cat}\nabla\varphi$$
$$N_{an} = -D_{an}\nabla c_{an} - u_{an}z_{an}Fc_{an}\nabla\varphi \quad (2)$$

Here, D are diffusion coefficients, F is the Faraday constant, and $z = +/-1$ the charge number. The mobilities u are determined by $u = D/(RT)$ (R: gas constant; T: temperature). Equation (1) and (2) are coupled via the space charge density ρ [Eq. (3)]:

$$\rho = F\,(z_{cat}c_{cat} + z_{an}c_{an}), \quad (3)$$

In the charged ionomer membrane with a fixed space charge density $z_{mem}c_{mem}$ it becomes [Eq. (4)]:

$$\rho = F\,(z_{cat}c_{cat} + z_{an}c_{an} + z_{mem}c_{mem}) \quad (4)$$

In this model, we assume ion transport exclusively by migration and diffusion; only steady-state gradients of the electric potential and the concentrations and no transient behavior are determined; the ionomer nanopore geometry is not modeled explicitly, and instead a homogenous 'space charge density' $z_{mem}c_{mem}$ is used in the ionomer (nanopores are very small [$\leq$2 nm diameter for Nafion] compared to all other features of the geometry). We further set the charge of all surfaces of the microhole membrane separating both reservoirs to 0 C m^{-2}, i.e., the electrical field is shielded from entering this membrane.

We employed finite element analysis (COMSOL Multiphysics 5.2) to model a two-dimensional axisymmetric (cylindrical symmetry) 6 μm long micropore with a 10 μm diameter, and a 10 μm thick and 200 μm wide ionomer deposit which extends 3 μm into the microhole. Potential differences of up to +/−0.5 V are applied between both ends of two 160 μm high and 320 μm wide reservoirs (see Supporting Information for details of the geometry). At the same surfaces, we couple to infinitely large reservoirs by setting constant equal concentrations of e.g., $c_{an} = c_{cat}$ =10 mM. The simulation directly yields the electric field as well as concentrations of cations and anions. We determined currents i as the sum of the ion fluxes of both types of ions normal to the pore cross section area: $i = F\int z_{an}N_{n,an} + z_{cat}N_{n,cat}$.

2.3. Current Rectification

Typical simulated rectification behavior for a 1 mM HCl concentration and a negative ionomer charge of 50 mM $-e^-$ is shown in Figure 3A (blue curve). At a voltage of 0.5 V, a current of 340 nA is reached, while it is reduced to −35 nA at a reverse bias of −0.5 V leading to a rectification ratio of 10. The black curve depicts the I–V characteristics for an open pore without any ionomer deposit. Also in good agreement with experiments,[23] here the forward current is *lower* for positive voltages. The *higher* conductivity of the film deposit compared to an open pore is caused by the high cation concentration there, which more than compensates for a reduced ion mobility. The used diffusion coefficients typical for Nafion and aqueous solvents are compared in Table 1.

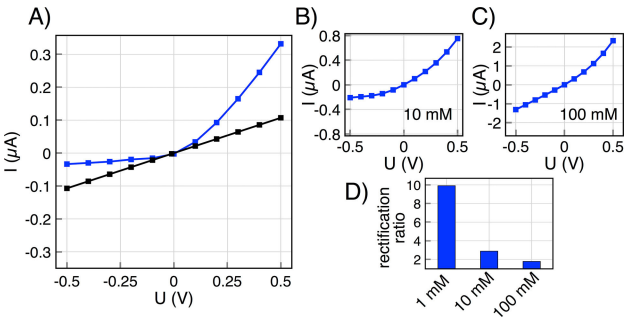

Figure 3. Simulated *I–V* curves and rectification in ionomer microhole deposits for an ionomer charge density of 50 mM $-e^-$ and HCl bulk concentrations (blue) of A) 1 mM, B) 10 mM, and C) 100 mM. The black curve in (A) shows the *I–V* for an open microhole without any deposit. (Lines are guides for the eye.) C) Rectification ratios at +/−0.5 V.

Figures 3B and C show that currents are increased for higher HCl electrolyte concentrations, but rectification is greatly reduced, an effect also observed experimentally.[23] In particular for 100 mM HCl, rectification is very small because the bulk electrolyte concentration exceeds the concentration of fixed ionomer charges. We note that, while we only show results for a 50 mM fixed negative charge concentration, currents scale linearly with increasing overall charge concentration, i.e., the magnitude of an I–V curve doubles when electrolyte and fixed charge concentrations are doubled.

The influence of the type of ions is shown in Figure 4. For Na^+ cations, which have a considerably smaller diffusion coefficient than protons, the current in reduced. However, the rectification ratio is increased as Na^+ ions are more efficiently blocked from entering the microhole in reverse bias. For both HCl and NaCl the current is almost exclusively determined by cations, it is about two orders of magnitude higher than the anion current due to the very low diffusivity of Cl^-, in particular in the ionomer membrane. For a hypothetical electrolyte with equal diffusivities of both types of ions in the membrane as well as in bulk, the anions would contribute to the overall current in forward bias (see Figure 4B). The contribution would be lower than the cation current as the anion concentration is much lower in the ionomer membrane, but the rectification ratio would be substantially higher.

Table 1. Diffusion coefficient in m^{2}s^{-1} employed in simulations. The ionomer diffusivities of H^+, Na^+ and Cl^- are typical for Nafion membranes.[30]

	$D(H^+)$	$D(Na^+)$	$D(Cl^-)$	uniform D
Ionomer	5.3×10^{-10}	1.6×10^{-10}	2.1×10^{-12}	1×10^{-9}
Reservoirs	8.1×10^{-9}	1.3×10^{-9}	2.0×10^{-9}	1×10^{-9}

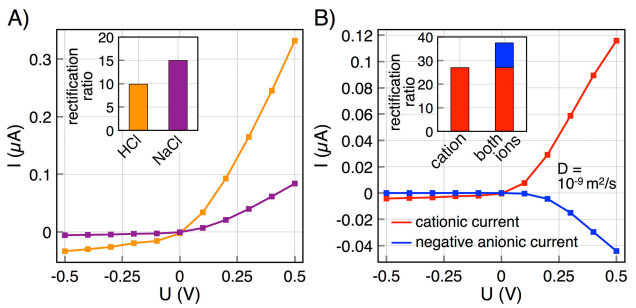

Figure 4. Comparison of diode switching for varying diffusivities for 1 mM electrolyte concentrations and 50 mM $-e^-$ fixed charges. A) *I–V* curves for HCl (orange) and NaCl (purple). B) *I–V* curves for electrolyte ions with $D = 10^{-9}\ m^2\ s^{-1}$ in the membrane and reservoirs. The contributions of cationic (red) and anionic (blue) ion fluxes are shown. Insets show the corresponding rectification ratios at +/−0.5 V, in (B) it shows the cationic (red) and cumulative (red and blue) ratio.

We determined the influence of the geometry of ionomer-microhole assemblies, i.e., microhole length and diameter, on the diode effect. I–V curves and rectification factors are shown in Figure 5 (for HCl diffusivities, 10 mM electrolyte and 50 mM fixed $-e^-$ charge concentrations.) A change in diameter leads to a change in the overall current, but *not* to a significant change in rectification. This is not surprising as concentration profiles in the microhole are constant in radial direction (see Supporting Information), and, thus, a smaller diameter does not lead to better ion confinement. In contrast, concentration profiles vary greatly along the height of the hole (see Figure 2C). Consequently, a longer microhole leads to a stronger confinement, more pronounced accumulation/depletion, and to a higher rectification as shown in Figure 5B. Experimentally, a somewhat reduced rectification was observed for wider microholes,[23] seemingly a discrepancy to the numerical results in Figure 5A. However, we believe that a wider microhole may also lead to a better filling of the microhole with the ionomer film. I.e., the film extends further into the hole, reducing the effective length, and, thus, the rectification. Therefore, in future better control of the "filling geometry" in experiments will be important.

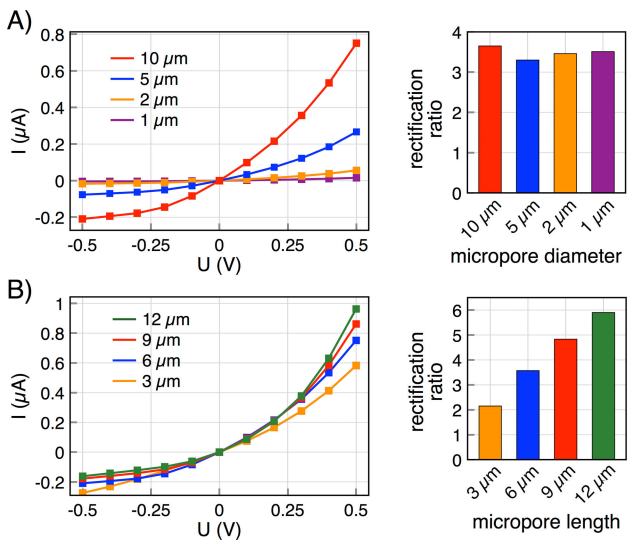

Figure 5. Comparison of the diode effect for varied geometries for a 10 mM electrolyte and 50 mM $-e^-$ fixed charge concentration, and HCl electrolyte diffusivities. A) *I–V* curves and rectification ratios at +/−0.5 V for microhole diameters ranging from 1 μm to 10 μm for a fixed microhole length of 6 μm. B) *I–V* curves and rectification ratios at +/−0.5 V for microhole lengths ranging from 3 μm to 12 μm for a fixed diameter of 10 μm.

We did not observe any change in the I–V curve for changing the ionomer film thickness (from 3 μm to 12 μm, data not shown). Such a change is not expected as ion concentrations are constant for a micrometer long segment across the film (see Figure 2C) in forward as well as reversed bias. Therefore, also a thin ionomer film yields efficient accumulation/depletion of ions in the microhole.

3. Conclusions

A simulation model for the treatment of microhole ionic rectifiers has been developed. This model provides both quantitative predictive information about the ionic diode performance as well as a qualitative model for the distribution of ions and for the conditions during operation of ionic diodes. In analogy to semiconductor diodes, ionomer-microhole deposits functionally differ from the p–n type junction of 'traditional' nanochannel diodes with segments of positive and negative surface charges. Instead, the rectifying depletion and accumulation of charge carriers takes place in an 'intrinsic' microhole without any significant fixed charges, i.e., they resemble a p–i or n–i junction instead. In this sense, ionomer-microhole deposits are closely related to nanoslots[27] and microchannel ionomer devices.[26]

Our model allows previous literature observations to be explained and in particular effects from electrolyte type and concentration to be verified. Most importantly, this model will now provide a tool for the prediction of better ionic diodes and of novel devices. As a further challenge the time dependence of the ionic diode switching process will be treated in the future.

Acknowledgements

B.D.B.A. is grateful for support from the Leverhulme Foundation (RPG-2014-308: "New Materials for Ionic Diodes and Ionic Photodiodes").

Conflict of Interest

The authors declare no conflict of interest.

Keywords: fluidic diode · Poisson-Nernst-Planck · desalination · iontronics

[1] P. Abgrall, N. T. Nguyen, *Anal. Chem.* **2008**, *80*, 2326–2341.
[2] K. Mathwig, Q. Chi, S. G. Lemay, L. Rassaei, *ChemPhysChem* **2016**, *17*, 452–457.
[3] H. Zhang, Y. Tian, L. Jiang, *Nano Today* **2016**, *11*, 61–81.
[4] M. Y. Kang, D. Momotenko, A. Page, D. Perry, P. R. Unwin, *Langmuir* **2016**, *32*, 7993–8008.
[5] Z. S. Siwy, S. Howorka, *Chem. Soc. Rev.* **2010**, *39*, 1115–1132.
[6] H. Daiguji, *Chem. Soc. Rev.* **2010**, *39*, 901–911.
[7] C. Wei, A. J. Bard, S. W. Feldberg, *Anal. Chem.* **1997**, *69*, 4627–4633.
[8] H. S. White, A. Bund, *Langmuir* **2008**, *24*, 2212–2218.
[9] N. Sa, W.-J. Lan, W. Shi, L. A. Baker, *ACS Nano* **2013**, *7*, 11272.
[10] I. Vlassiouk, Z. S. Siwy, *Nano Lett.* **2007**, *7*, 552–556.
[11] R. Karnik, C. Duan, K. Castelino, H. Daiguji, A. Majumdar, *Nano Lett.* **2007**, *7*, 547–551.
[12] B. Lovrecek, A. Despic, J. O. M. Bockris, *J. Phys. Chem.* **1959**, *63*, 750–751.
[13] E. Madrid, M. A. Buckingham, J. M. Stone, A. T. Rogers, W. J. Gee, A. D. Burrows, P. R. Raithby, V. Celorrio, D. J. Fermin, F. Marken, *Chem. Commun.* **2016**, *52*, 2792–2794.
[14] R. Zhao, G. H. He, Y. L. Deng, *Electrochem. Commun.* **2012**, *23*, 106–109.
[15] Y. Rong, A. Kolodziej, E. Madrid, M. Carta, R. Malpass-Evans, N. B. McKeown, F. Marken, *J. Electroanal. Chem.* **2016**, *779*, 241–249.
[16] Y. Rong, Q. Song, K. Mathwig, E. Madrid, D. He, R. G. Niemann, P. J. Cameron, S. E. Dale, S. Bending, M. Carta, et al., *Electrochem. Commun.* **2016**, *69*, 41–45.
[17] M. Lepoitevin, B. Jamilloux, M. Bechelany, E. Balanzat, J. M. Janot, S. Balme, *RSC Adv.* **2016**, *6*, 32228–32233.
[18] H. G. Chun, T. D. Chung, in R. G. Cooks, J. E. Pemberton, eds. , *Annual Review of Analytical Chemistry* **2015**, *8*, 441–462.
[19] W. J. Lan, M. A. Edwards, L. Luo, R. T. Perera, X. J. Wu, C. R. Martin, H. S. White, *Acc. Chem. Res.* **2016**, *49*, 2605–2613.
[20] P. Ramirez, V. Gomez, J. Cervera, S. Nasir, M. Ali, W. Ensinger, Z. Siwy, S. Mafe, *RSC Adv.* **2016**, *6*, 54742–54746.
[21] E. Madrid, P. Cottis, Y. Rong, A. T. Rogers, J. M. Stone, R. Malpass-Evans, M. Carta, N. B. McKeown, F. Marken, *J. Mater. Chem. A* **2015**, *3*, 15849–15853.
[22] E. Madrid, Y. Rong, M. Carta, N. B. McKeown, R. Malpass-Evans, G. A. Attard, T. J. Clarke, S. H. Taylor, Y.-T. Long, F. Marken, *Angew. Chem.* **2014**, *126*, 10927–10930.
[23] D. He, E. Madrid, B. D. Aaronson, L. Fan, J. Doughty, K. Mathwig, A. M. Bond, N. B. McKeown, F. Marken, *ACS Appl. Mater. Interfaces* **2017**, *9*, 11272–11278.
[24] B. D. Aaronson, D. He, E. Madrid, M. A. Johns, J. L. Scott, L. Fan, J. Doughty, M. A. Kadowaki, I. Polikarpov, N. B. McKeown, et al., *ChemistrySelect* **2017**, *2*, 871–875.
[25] L. Benson, L. H. Yeh, T. H. Chou, S. Z. Qian, *Soft Matter* **2013**, *9*, 9767–9773.
[26] G. Sun, S. Senapati, H.-C. Chang, *Lab. Chip* **2016**, *16*, 1171–1177.
[27] G. Yossifon, P. Mushenheim, Y.-C. Chang, H.-C. Chang, *Phys. Rev. E* **2009**, *79*, 046305.
[28] S. W. Park, G. Yossifon, *Phys. Rev. E* **2016**, *93*, 062614.
[29] Y. Green, Y. Edri, G. Yossifon, *Phys. Rev. E* **2015**, *92*, 033018.
[30] I. A. Stenina, P. Sistat, A. I. Rebrov, G. Pourcelly, A. B. Yaroslavtsev, *Desalination* **2004**, *170*, 49–57.
[31] I. Vlassiouk, S. Smirnov, Z. Siwy, *Acs Nano* **2008**, *2*, 1589–1602.
[32] W. Guan, R. Fan, M. A. Reed, *Nat. Commun.* **2011**, *2*, 506.

Manuscript received: May 13, 2017
Accepted Article published: July 19, 2017
Version of record online: August 10, 2017

Supporting Information

Simulation Geometry

The geometry of the simulated ionomer, microhole and reservoirs is shown in Figure 1S. We employ a two-dimensional cylindrical geometry; the rotational symmetry axis is positioned in the center of the pore. Electrical potentials are applied at the entire face surfaces of the reservoir cylinders. These surfaces also couple to infinitely large reservoirs, i.e., the electrolyte concentrations on the face surfaces are kept constant at 1, 10 or 100 mM, respectively. The horizontal green line on the right figure indicates microhole cross section; ions fluxes are integrated over this line/area to determine currents. The vertical green line depicts the position of the profiles shown in Figures 2B-D in the main text.

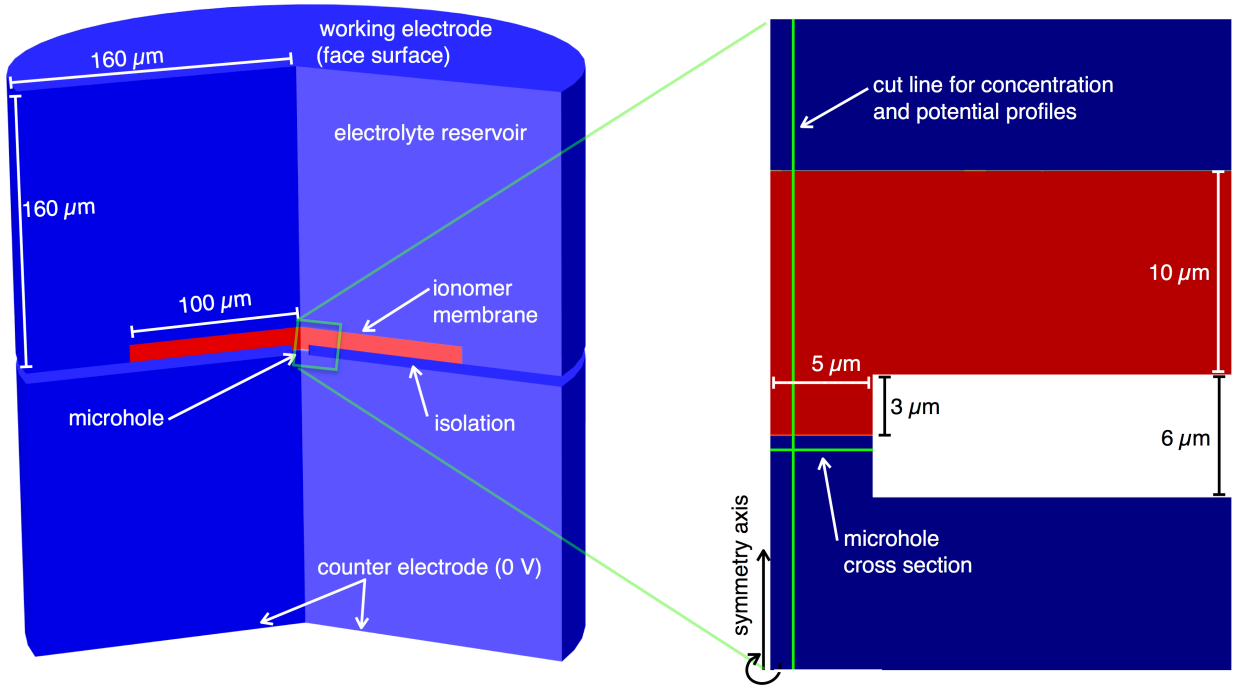

Figure S1. Left: 3D projection and dimensions of the 2D axisymmetric simulation geometry. The right figure zooms in on the ionomer and microhole in the 2D geometry.

Concentration profiles and potential gradients

Figures S2 and S3 show the potential and ion distributions in forward (0.5 V) and reverse bias (-0.5 V) for 50 mM fixed -e^- ionomer charges and a 1 mM HCl electrolyte concentration. These distributions correspond directly to the one-dimensional graphs in Figure 2 in the main text.

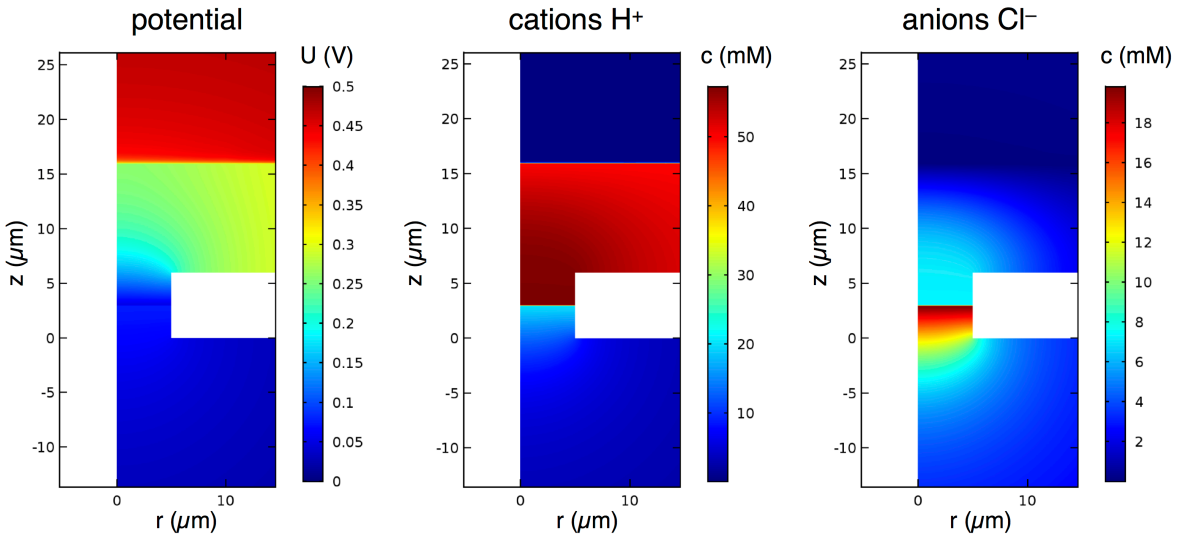

Figure S2. Potential and cation and anion distribution in an ionomer deposit in forward bias.

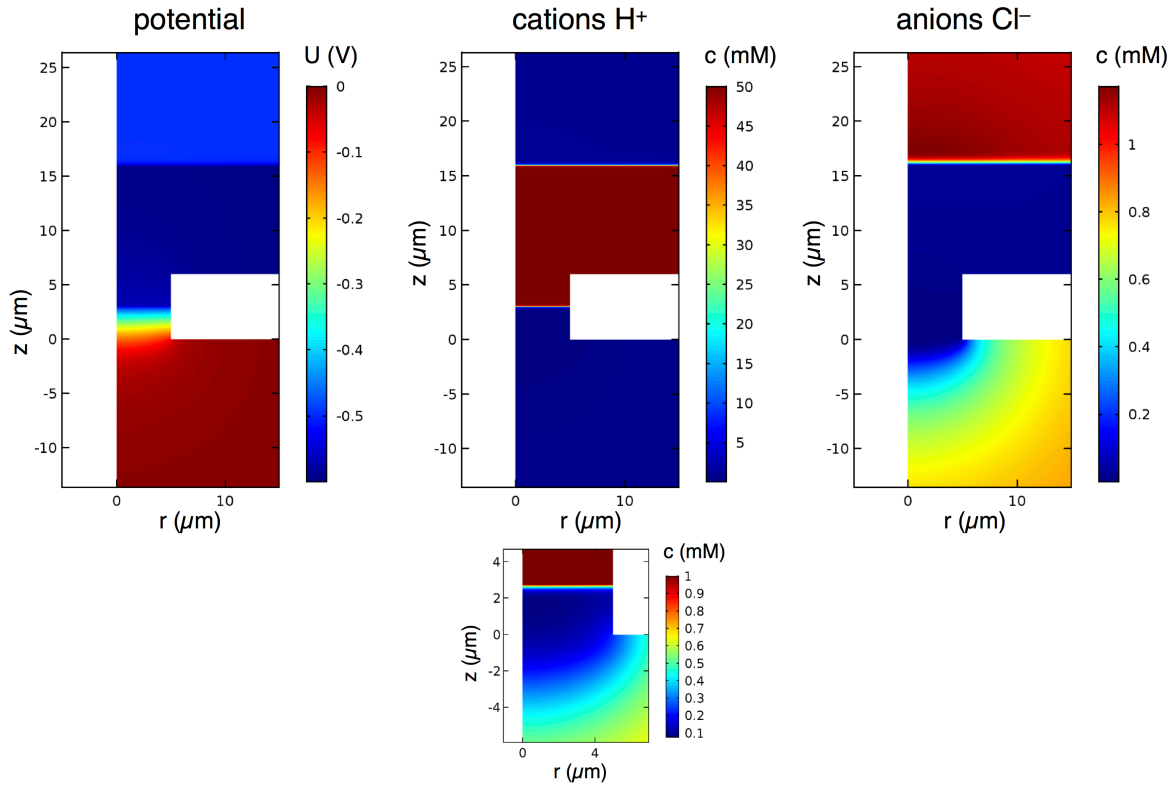

Figure S3. Potential and cation and anion distributions in an ionomer deposit in reverse bias. The figure below zooms in on the H^+ concentration in the microhole, only a 0.1 to 1 mM range is shown.